Role of Perivascular Oligodendrocyte Precursor Cells in Angiogenesis After Brain Ischemia

Natsue Kishida, MD; Takakuni Maki, MD, PhD; Yasushi Takagi, MD, PhD; Ken Yasuda, MD; Hisanori Kinoshita, MD; Takashi Ayaki, MD, PhD; Takayuki Noro, MD; Yusuke Kinoshita; Yuichi Ono, PhD; Hiroharu Kataoka, MD, PhD; Kazumichi Yoshida, MD, PhD; Eng H. Lo, PhD; Ken Arai, PhD; Susumu Miyamoto, MD, PhD; Ryosuke Takahashi, MD, PhD

Background—Oligodendrocyte precursor cells (OPCs) regulate neuronal, glial, and vascular systems in diverse ways and display phenotypic heterogeneity beyond their established role as a reservoir for mature oligodendrocytes. However, the detailed phenotypic changes of OPCs after cerebral ischemia remain largely unknown. Here, we aimed to investigate the roles of reactive OPCs in the ischemic brain.

Methods and Results—The behavior of OPCs was evaluated in a mouse model of ischemic stroke produced by transient middle cerebral artery occlusion in vivo. For in vitro experiments, the phenotypic change of OPCs after oxygen glucose derivation was examined using a primary rat OPC culture. Furthermore, the therapeutic potential of hypoxic OPCs was evaluated in a mouse model of middle cerebral artery occlusion in vivo. Perivascular OPCs in the cerebral cortex were increased alongside poststroke angiogenesis in a mouse model of middle cerebral artery occlusion. In vitro RNA-seq analysis revealed that primary cultured OPCs increased the gene expression of numerous pro-angiogenic factors after oxygen glucose derivation. Hypoxic OPCs secreted a greater amount of pro-angiogenic factors, such as vascular endothelial growth factor and angiopoietin-1, compared with normoxic OPCs. Hypoxic OPC-derived conditioned media increased the viability and tube formation of endothelial cells. In vivo studies also demonstrated that 5 consecutive daily treatments with hypoxic OPC-conditioned media, beginning 2 days after middle cerebral artery occlusion, facilitated poststroke angiogenesis, alleviated infarct volume, and improved functional disabilities.

Conclusions—Following cerebral ischemia, the phenotype of OPCs in the cerebral cortex shifts from the parenchymal subtype to the perivascular subtype, which can promote angiogenesis. The optimal use of hypoxic OPCs secretome would provide a novel therapeutic option for stroke. (***J Am Heart Assoc.*** 2019;8:e011824. DOI: 10.1161/JAHA.118.011824.)

Key Words: angiogenesis • glial cell • stem cell • stroke

S troke is the leading cause of adult neurological disability globally. Although progress has been made in stroke research, most translational efforts aimed at developing

From the Departments of Neurology (N.K., T.M., K.Y., H.K., T.A., T.N., R.T.), and Neurosurgery (N.K., Y.T., H.K., K.Y., S.M.), Graduate School of Medicine, Kyoto University, Kyoto, Japan; Department of Neurosurgery, Graduate School of Medicine, Tokushima University, Tokushima, Japan (Y.T.); Department of Developmental Neurobiology, KAN Research Institute, Inc., Kobe, Japan (Y.K., Y.O.); Departments of Radiology and Neurology, Massachusetts General Hospital and Harvard Medical School, Charlestown, Massachusetts, USA (E.H.L., K.A.).

Correspondence to: Takakuni Maki, MD, PhD, Department of Neurology, Graduate School of Medicine, Kyoto University, 54 Shogoin-Kawahara-cho, Sakyo-ku, Kyoto, Japan. E-mail: harutoma@kuhp.kyoto-u.ac.jp

Received January 6, 2019; accepted March 21, 2019.

effective therapies have failed, except for thrombolytic therapy or intravascular thrombectomy that only benefit a small proportion of patients. Recent research has shifted from a purely neurocentric view to a more integrated view that embraces the well-accepted concept of the neurovascular unit, which proposes that dynamic interactions among all cell types contribute to function and dysfunction in the brain.[1] Additionally, a damaged brain is plastic and exhibits dual responses after injury: a destructive response during the acute phase and a self-restorative response during the chronic phase.[2] Thus, a deeper understanding of neurovascular injury and repair mechanisms following stroke would lead to novel therapeutic approaches, which may suppress detrimental processes and promotes endogenous regenerative responses.[3]

Among the cell types involved in the neurovascular unit, oligodendrocyte precursor cells (OPCs) are widely dispersed throughout the adult vertebrate brain and have been shown to play more diverse and crucial roles than previously

ORIGINAL RESEARCH

Clinical Perspective

What Is New?

- Oligodendrocyte precursor cells in cerebral cortex shifts to perivascular subtype with pro-angiogenic traits after ischemia.

What Are the Clinical Implications?

- Hypoxic oligodendrocyte precursor cells may provide a novel therapeutic option for ischemic stroke.

appreciated.[4] In addition to serving as a reservoir for mature oligodendrocytes, which form myelin sheaths, OPCs regulate neuronal, glial, and vascular systems in a direct and reciprocal fashion. As with other glial cells (ie, microglia and astrocytes),[5,6] OPCs are not homogeneous, but heterogeneous, and have various phenotypes, exerting multifaceted roles under normal and pathological conditions. The OPCs and oligodendrocytes in different regions of the brain exist in distinct subpopulations in terms of molecular, electrophysiological, and functional properties, as well as their transcriptional gene expression profiles.[4,7] In addition to these regional variations, there are 3 subtypes of OPCs: perivascular, parenchymal, and intermediate, which are classified based on their spatial relation to the brain's microvasculature.[8–10] Although their functional differences have not been fully elucidated, it is known that perivascular OPCs, situated in proximity to microvasculature, wrap microvessels with their fine processes, while parenchymal OPCs are situated away from microvessels.

Following central nervous system injury, the OPCs may play both detrimental and beneficial roles, responding to various types of pathological insults in different locations in the brain. Although extrinsic signals can trigger a wide range of intrinsic changes in OPCs in an injury- or disease-specific manner, the detailed phenotypic changes of OPCs after cerebral ischemia remain largely unknown. Thus, the purpose of this study is to elucidate how OPCs contribute to neurovascular damage and regeneration following stroke and investigate the role of reactive OPCs in the ischemic brain.

Materials and Methods

The authors declare that all the supporting data are available within the article.

Animals

All experimental procedures were approved and performed in accordance with the institutional Animal Care and Use Committee of Kyoto University. C57BL/6N male mice aged 11 to 13 weeks and weighing 22 to 28 g were used.

Transient Focal Cerebral Ischemia

Cerebral ischemia was induced using the standard intraluminal middle cerebral artery occlusion (MCAO) method as described previously.[11] Mice were anesthetized with isoflurane in 50% N_2O and 50% O_2 mixture. Rectal temperature was maintained at 36.5°C to 37.9°C using a heating pad and lamp. After a middle skin incision was made, the left common carotid artery was exposed. The MCAO was established by inserting a 0.21- or 0.22-mm filament (Doccol) from the left common carotid artery to the origin of the MCA. After 40 minutes of MCAO, reperfusion was established by removing the filament. Regional cerebral blood flow was measured with a laser-Doppler flowmetry (Omegawave, Tokyo, Japan) to confirm the induction of ischemia and reperfusion. The surgical procedures were considered successful as >80% reduction from baseline throughout ischemia. Exclusion criteria, set before the experiment, were as follows: (1) animals died of anesthetic or procedural problems during surgeries; (2) animals died before sampling after surgery; (3) animals did not achieve a reduction of MCA blood flow measured by laser-Doppler flowmetry during MCAO; and (4) animals did not achieve reperfusion.

Immunohistochemistry

Mouse brains were collected after perfusion with PBS (phosphate-buffered saline) and 4% PFA (paraformaldehyde). Brain sections were fixed with 4% PFA and 20% sucrose. Brain sections were rinsed with PBS. After blocking with 3% BSA (bovine serum albumin), sections were incubated at 4°C overnight in 0.3% BSA solution containing primary antibodies, anti-platelet-derived growth factor receptor-α (PDGFRα) (1:200; R and D Systems), anti-microtubule-associated protein 2 (1:500, Sigma-Aldrich), anti-GFAP (glial fibrillary acidic protein) (1:400, Invitrogen), anti-Ki67 (1:200, Invitrogen), anti-CD31 (1:200; BD Pharmingen), anti-glucose transporter-1 (GLUT1) rabbit pAb (1:200, Calbiochem), anti-Iba-1 (1:200, Wako), anti-CD140b (1:200, eBioscience), anti-NG-2 (1:200, Chemicon), anti-Nestin (1:200, Abcam), and anti-fibronectin (1:200, Dako) at 4°C overnight. After washing with PBS, sections were incubated with secondary antibodies conjugated with fluorescein isothiocyanate, Texas Red, or Cy5 (1:200, Alexa Fluor 488, 594, and 647) for 1 hour at room temperature. After washing with PBS, the cells were covered with VECTASHIELD mounting medium (Vector Laboratories) with 4′,6-diamidino-2-phenylindole (DAPI). A terminal deoxynucleotidyl transferase dUTP nick end labeling (TUNEL) assay was performed to identify apoptotic cells, according to the manufacturer's protocol (Promega). The sections were observed using an Olympus Fluoview FV1000 confocal microscope (Olympus, Japan) or KEYENCE. Using a confocal laser-scanning microscope (FV1000) with an objective lens (40×, NA 0.95), a z-stack of images (512×512 pixels; 0.621 μm/pixels; 3.0 μm z-step) was acquired.

Blood–Brain Barrier Permeability

Blood–brain barrier (BBB) disruption after ischemia was evaluated using IgG staining. For IgG staining, sections were incubated overnight at 4°C with an antibody against donkey anti-mouse IgG (1:300, Jackson ImmunoResearch Laboratories). A total of 3 coronal sections (+1, 0.5, and 0 mm from Bregma) were chosen for IgG leakage quantification. We took photographs from 2 areas in the ischemic border area under a 20× objective. The IgG fluorescent intensity was quantified using ImageJ software.

Vascular Density Assessments

Coronal sections (20 μm thick) were stained with anti-GLUT-1 (1:200) or anti-CD31 (1:200). A total of 3 coronal sections (+1, 0.5, and 0 mm from bregma) were chosen for vascular quantification. We took photographs from 2 areas in the border area under a 20× objective. The branch number and GLUT-1 fluorescent intensity were quantified using ImageJ software.

Measurement of Infarct Volume

Coronal brain sections were separated by 20-μm intervals at various coronal levels. A total of 6 sections (+3.0, +2.0, +1.0, 0, −1.0, and −2.0 mm from bregma) were stained with crystal violet. Images were taken with a fluorescence microscope (KEYENCE BZ-X 710) by an investigator who was blinded to the experimental groups. The images were exported into ImageJ software in TIFF format. The areas of the contralateral hemisphere (A) and the ipsilateral hemisphere without infarct (B) on each section were measured using ImageJ software. The infarct areas were calculated by (A-B). Measurements were multiplied by the distance between sections (1 mm) and then summed over the entire brain to yield the volume measurements.

Behavioral Measurements

Neurological severity score

Neurological severity score was tested on day 2 and day 7 after MCAO, as described previously.[11] The score was defined as follows: 0 = no observable neurological deficit; 1 = failure to extend the right forelimb; 2 = circling to the contralateral side; 3 = no spontaneous movement and/or inability to maintain upright posture.

Corner test

The corner test evaluated sensorimotor asymmetry, as described previously.[12] The mice were placed in a corner with an angle of 30°. To exit the corner, the mouse could turn to the left or right and this choice was recorded. The test was repeated 10 times, with at least 30 seconds between trials, and the percentage of left turns was calculated. Only turns involving full rearing along either wall were included.

Garcia score

The Garcia score, an 18-point scoring system, was used as previously described.[13]

Six aspects of neurological deficits, including (1) spontaneous activity, (2) symmetry in the movement of the 4 limbs, (3) forepaw outstretching, (4) climbing ability, (5) body proprioception, and (6) response to vibrissae touch were measured. Each aspect was scored on a scale between 0 and 3 points, and a total score was calculated. All behavioral tests were conducted in a quiet room.

Rota-rod test

The rota-rod test was performed on day 7 after MCAO. Mice were placed on an accelerating rota-rod apparatus (UGO-Basile model 7650, Italy), wherein the speed increased from 0 to 40 rpm over 4 minutes. The time for which the mice could remain on the rotating cylinder was measured. Two trials were performed and the average time periods were analyzed.

Sholl analysis

A Sholl analysis method was developed to distinguish between the perivascular and parenchymal types in the immunofluorescent images of the brain.[14] PDGFRα (+) OPCs were 3-dimensionally reconstructed using confocal images and Neurolucida software version 10 (MBF-Bioscience, Williston, ND). The reconstructions of OPCs were drawn over a live picture on a PC. By using Neurolucida Explorer, a Neurolucida software extension, each reconstructed OPC was assessed. The center of the cell body was used as a reference point and concentric circles were drawn at an interval of 10 μm. The number of intersections was analyzed for all the 10-μm, 20-μm, 30-μm, and 40-μm concentric circles. Total dendritic length and total intersections were also analyzed.

Immunostaining of Hypoxyprobe™-1

Hypoxyprobe™-1 was evaluated for tissue hypoxia.[12] The brains were evaluated 24 hours after intraperitoneal injection of Hypoxyprobe™-1 (60 mg/kg). The sections were rinsed and incubated overnight at 4°C with mouse monoclonal anti-pimonidazole antibody (Mab1), and diluted in PBS containing 0.3% BSA (1:200). Subsequently, after washing with PBS, the sections were incubated with secondary antibodies conjugated with Texas Red (1:200, Alexa Fluor 594) for 1 hour at room temperature. After washing with PBS, the sections were covered with VECTASHIELD mounting medium (Vector Laboratories) with DAPI.
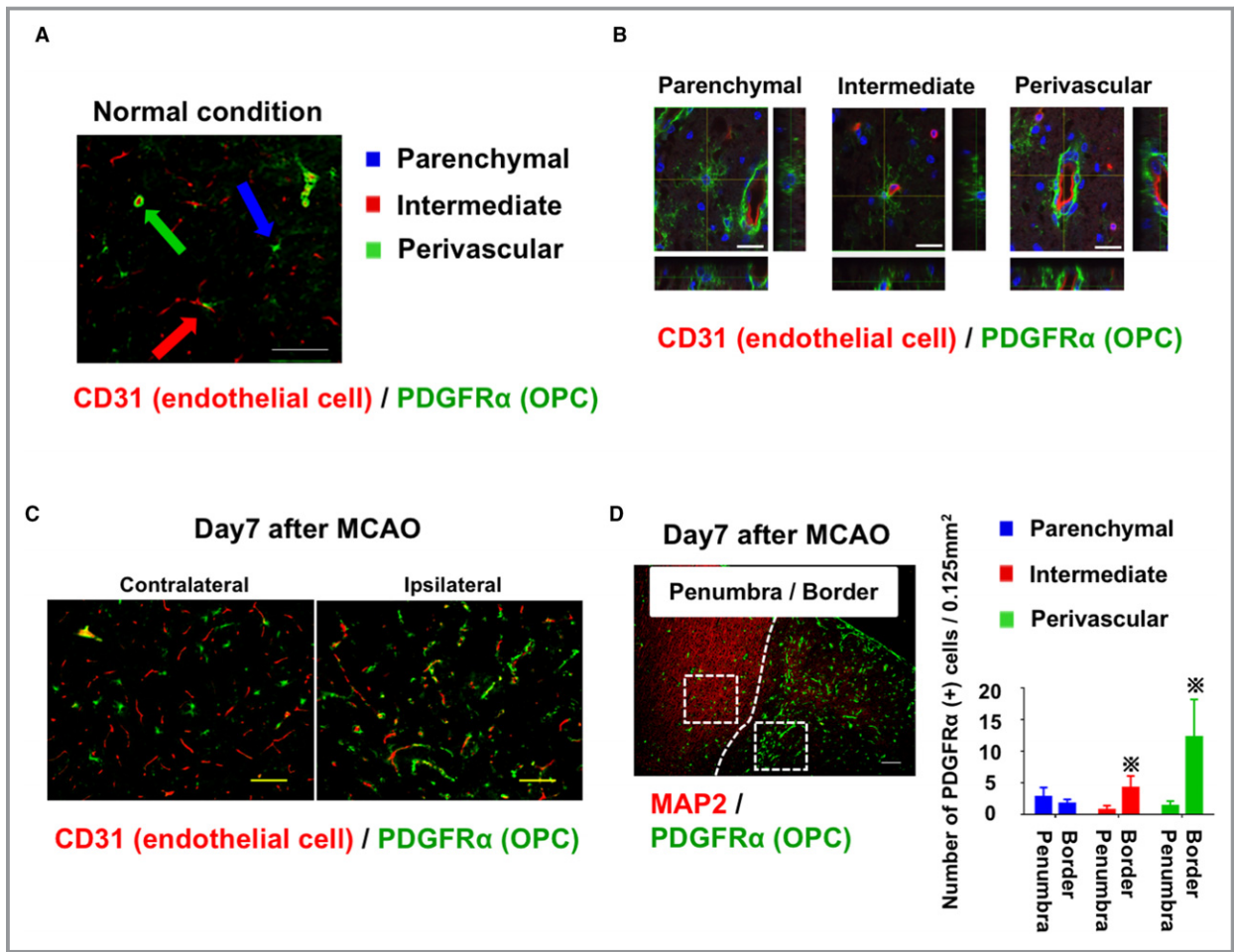
Figure 1. Perivascular OPCs in the cerebral cortex are increased at the ischemic border area after MCAO in vivo. **A**, Representative image of PDGFRα (green: marker for OPCs) and CD31 (red: marker for endothelium) immunostaining in the cerebral cortex under normal conditions. There are 3 subtypes of OPCs: parenchymal, intermediate, and perivascular type. Bar=100 μm. **B**, Representative image of PDGFRα (green) and CD31 (red) immunostaining with 4′,6-diamidino-2-phenylindole (blue: marker for nuclei) of the cerebral cortex in a 3-dimensional image using a confocal laser-scanning microscope. Bar=20 μm. **C**, Representative images of PDGFRα and CD31 immunostaining at the ischemic border and contralateral areas on day 7 after MCAO. Bar=100 μm. **D**, Histogram showing quantification of PDGFRα (+) cell numbers in penumbra and ischemic border areas on day 7 after MCAO. Data are expressed as the mean±SD. Data are analyzed using a Mann–Whitney test. N=4 for each group. $P<0.05$. Bar=100 μm. **E**, Representative immunofluorescent images of PDGFRα (green: marker for OPCs) and Mab1 (red: hypoxic probe) on day 7 after MCAO. Bar=100 μm. **F**, Representative immunofluorescent images of PDGFRα (marker for OPCs), Nestin (marker for neural stem cells), Iba-1 (marker for microglia), PDGFRβ (marker for pericytes), GFAP (marker for astrocytes), and Col-1 (marker for fibroblast), in the ischemic border areas. Bar=100 μm. GFAP, glial fibrillary acidic protein; MCAO, middle cerebral artery occlusion; OPCs, oligodendrocyte precursor cells; PDGFRα, platelet-derived growth factor receptor-α.

Primary Oligodendrocyte Lineage Cell and Endothelial Cell Culture

OPCs were prepared as previously described.[15,16] Briefly, cerebral cortices from 1- to 2-day-old Sprague Dawley rats (Shimizu Laboratory Supplies Co, Ltd) were dissected, minced, and digested. Dissociated cells were plated in poly-D-lysine-coated 75-cm² flasks, and maintained in DMEM (Dulbecco's modified Eagle medium) containing 20% heat-inactivated fetal bovine serum and 1% penicillin/streptomycin. After the cells

were confluent (≈10 days), the flasks were shaken for 1 hour on an orbital shaker (220 rpm) at 37°C to remove microglia. The flasks were then filled with a new medium and shaken overnight (≈20 hours). The medium was collected and plated on noncoated tissue culture dishes for 1 hour at 37°C to eliminate contaminating astrocytes and microglia. The nonadherent cells (ie, OPCs) were collected and replated at a density of 20,000 cells/cm² in Neurobasal (NB) medium containing 2 mmol/L glutamine, 1% penicillin/streptomycin, 10 ng/mL PDGF-AA, 10 ng/mL FGF-2, and 2% B27
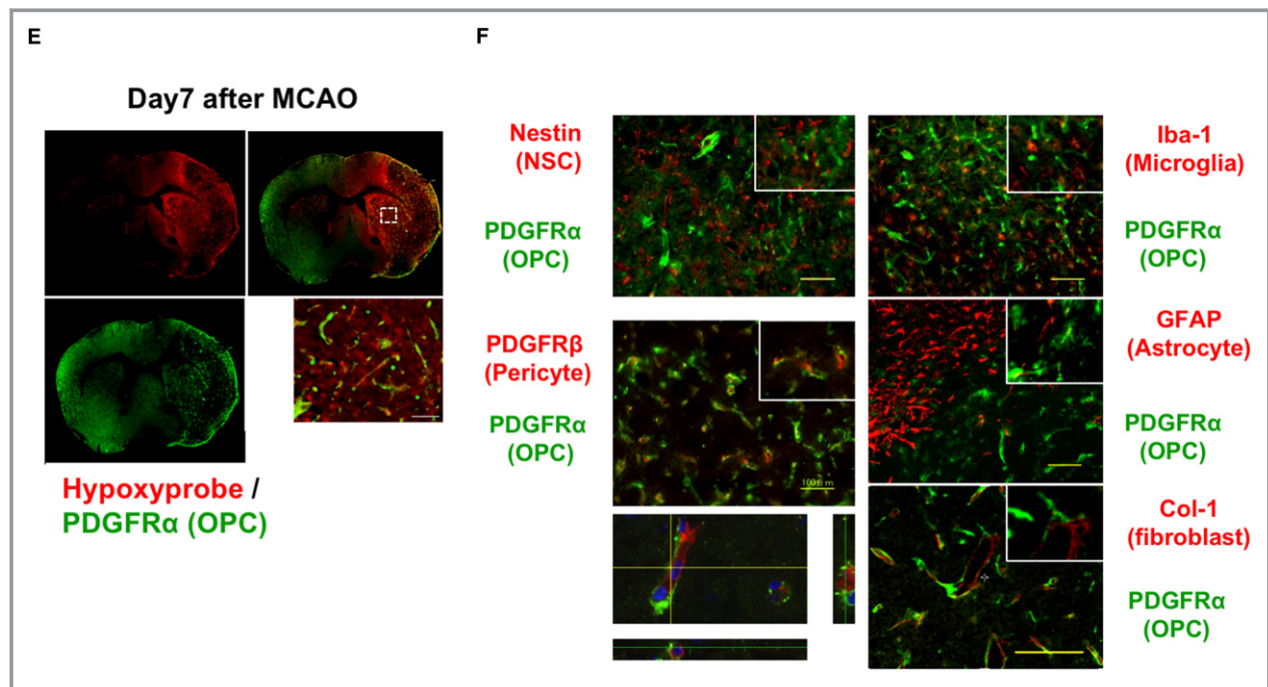
Figure 1. Continued

supplement onto poly-DL-ornithine-coated plates. Four to 6 days after plating, the OPCs were used for the experiments. Human Brain Microvascular Endothelial Cells (Cell Systems) were cultured in EBM-2 (Lonza, NJ) containing EGM-2MV single quots kit (Lonza) onto collagen-coated flasks (BD Biosciences, CA).

Preparation of Oligodendrocyte Lineage Cell Conditioned Media

The conditioned media (CM) was prepared, as described previously.[17] Cell cultures were washed with PBS and maintained in basal media without fetal bovine serum and growth supplement for 12 hours under normoxic (21% oxygen) and hypoxic (2% oxygen) conditions. CM was then collected and centrifuged at 10 000g for 5 minutes at 4°C to remove cells and debris. The CM was concentrated using 5 kDa-membrane centrifuge tubes (Sartorius, V0601) and spun for a total of 22 minutes at 4000g at 21°C (about 5× final volume). The CM was stored at −80°C until use.

In Vitro Vessel Formation Assay

The standard Matrigel assay (in vitro angiogenesis assay) was used to assess the spontaneous formation of capillary-like structures by the endothelial cells. Standard 15-well plates were coated with 12 μL of cold Matrigel and left to solidify at 37°C for 30 minutes. Cells (2×10^5 cells/mL)

were seeded into the plates and incubated at 37°C for 18 hours with different conditions. For the media transfer experiments, hypoxic OPC-CM and basal media were diluted with EBM-2 at a ratio of 50:50. The degree of tube formation was determined by counting the number of tubes in 5 random fields from each well under a ×10 objective magnification.

Assessment of Cell Proliferation With WST Assay

Cell proliferation/survival was assessed by the WST reduction assay kit (Cell Counting Kit-8, Dojindo). WST assay is a sensitive colorimetric method used to detect cell viability. Cells were incubated with 10% WST solution for 1 hour at 37°C and then the absorbance of the each medium (DMEM, OPC-CM, and hypoxic OPC-CM) was measured using a microplate reader with a test wavelength of 450 nm and a reference wavelength of 630 nm.

RNA-seq Analysis in OPCs

RNA-seq library construction and sequencing

Agilent SureSelect Strand Specific RNA prep kit (Cat# G9691A) was used with 200 ng of total RNA for the construction of cDNA libraries according to the manufacturer's protocol. All cDNA libraries were sequenced using an Illumina Miseq, producing 76×2 bp paired-end reads with multiplexing.
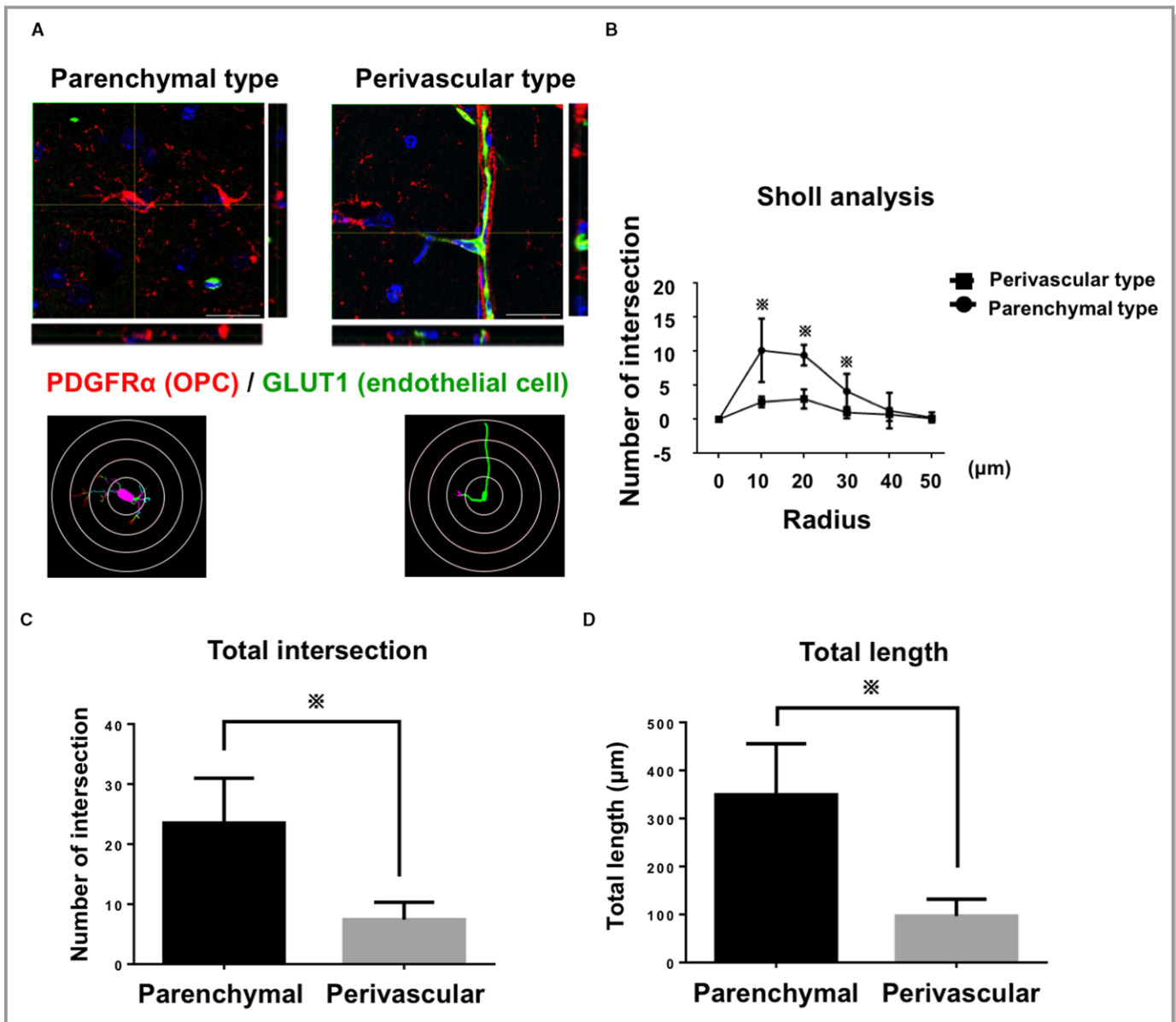
Figure 2. Sholl analysis demonstrates distinct morphological differences between parenchymal and perivascular OPCs. **A**, Representative images of PDGFRα (+) parenchymal and perivascular OPCs (red) and endothelial cells (green). Bar=20 μm. Lower panels show the reconstructions of OPCs drawn over a live picture on a PC. **B**, Histogram showing the number of intersections with the concentric circles around the soma of the OPCs plotted against the radius of the spheres. **C** and **D**, Histogram showing the intersection (**C**) and total length (**D**) of parenchymal and perivascular OPCs. N=7 for each group. Data are analyzed using a Mann–Whitney test. *P*<0.05. GLUT-1 indicates glucose transporter 1; OPCs, oligodendrocyte precursor cells; PDGFRα, platelet-derived growth factor receptor-α.

Bioinformatics analysis

All raw sequencing reads were trimmed using Trimmomatic software.[18] Bases and QC assessment of sequencing were generated using FastQC. QC-passed reads were aligned to the Ensembl Rnor 6.0.84 reference genome using Star v2.5.0c.[19] The abundance of transcripts was then estimated using an Expectation-Maximization algorithm implemented in the software package Cufflnk v2.2.1 (http://cole-trapnell-lab.github.io/cufflinks/). Drawing heatmap of the RNA-seq data was performed using R software and the ggplot2 package.

Statistical Analysis

All quantitative data were statistically analyzed using GraphPad prism software version 5.0 (GraphPad software Inc) and Stata 14 (STATA corp, College Station). Because the sample sizes were small and normal distribution cannot be
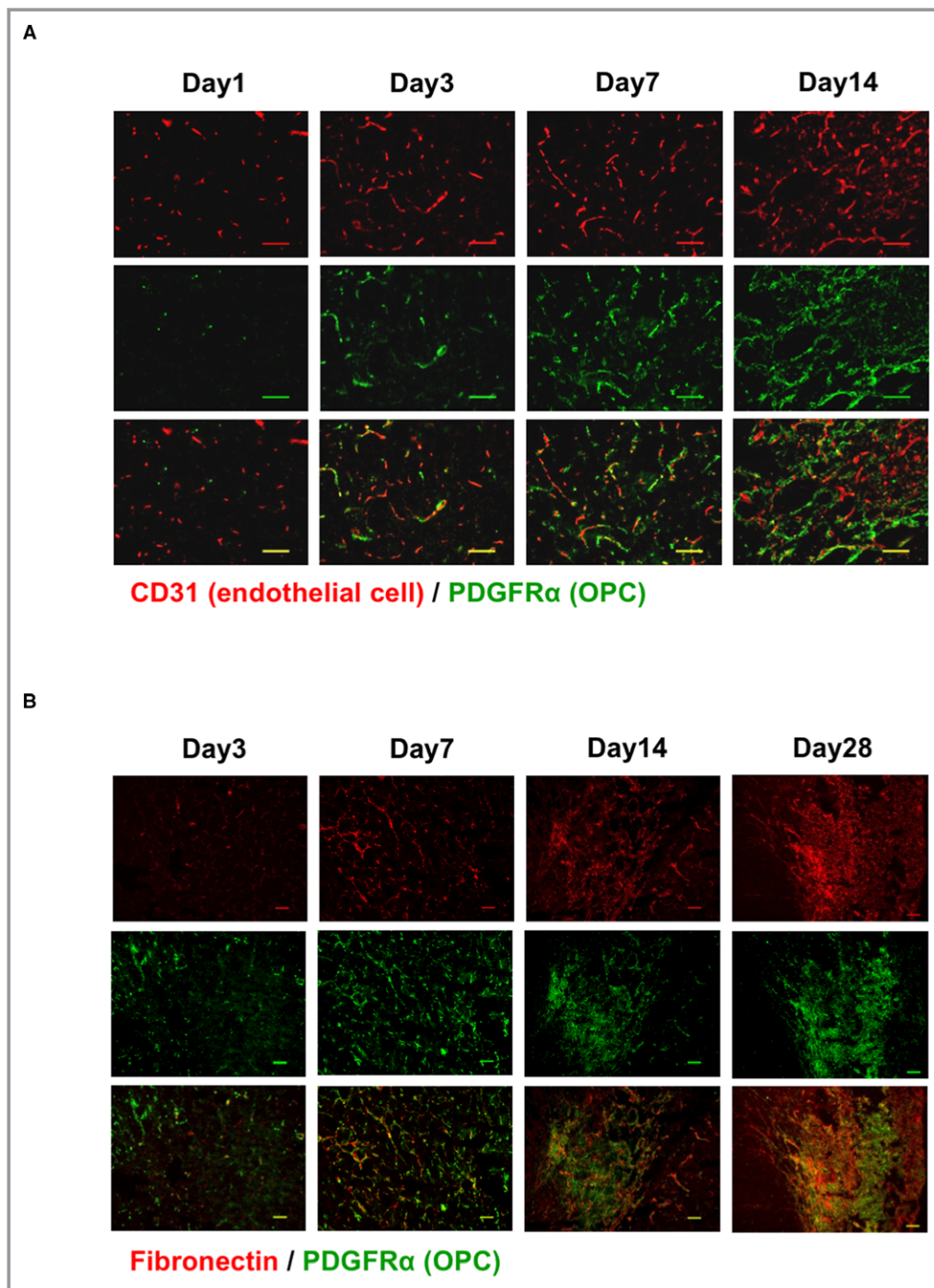
Figure 3. Perivascular OPCs in the cerebral cortex, at the ischemic border area, are increased concomitantly with increased angiogenesis after middle cerebral artery occlusion (MCAO) in vivo. **A**, Representative images of PDGFRα and CD31 immunostaining at the ischemic border area 1, 3, 7, and 14 days after MCAO. Bar=100 μm. **B**, Representative images of PDGFRα and fibronectin immunostaining at the ischemic border area 3, 7, 14, and 28 days after MCAO. Bar=100 μm. MCAO indicates middle cerebral artery occlusion; OPCs, oligodendrocyte precursor cells; PDGFRα, platelet-derived growth factor receptor-α.

guaranteed in continuous variables, nonparametric tests were conducted. Mann–Whitney U test was used to compare continuous variables between 2 groups and Fisher exact test was used to compare categorical variables in neurological severity score. Kruskal–Wallis test was used for comparing continuous variables among 3 or more groups, followed by
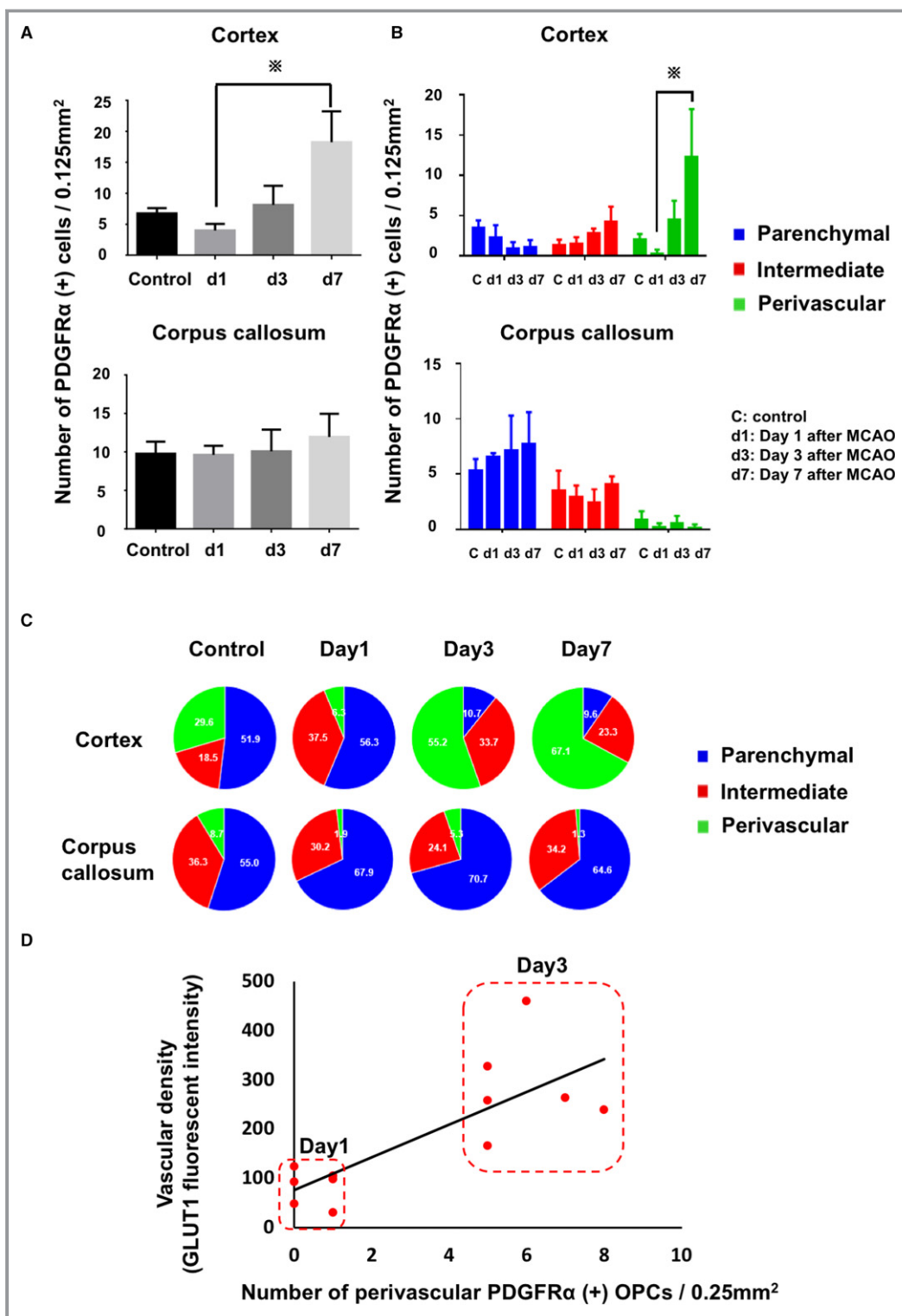
Figure 4. Perivascular OPCs in the cerebral cortex, at the ischemic border area, are increased concomitantly with increased angiogenesis after MCAO in vivo. **A** through **C**, Histogram showing the total numbers of PDGFRα (+) cells in the cortex and corpus callosum (**A**), and the number (**B**) and proportion (**C**) of the 3 subtypes. Data are expressed as the mean ±SD. Data are analyzed using a Kruskal–Wallis test. N=6 for each subtype. $P<0.05$. **D**, The correlation between the number of perivascular PDGFRα (+) OPCs and vascular density demonstrates significant linear correlation ($r=0.7827$, $P<0.01$). GLUT1 indicates glucose transporter 1; MCAO indicates middle cerebral artery occlusion; OPCs, oligodendrocyte precursor cells; PDGFRα, platelet-derived growth factor receptor-α.
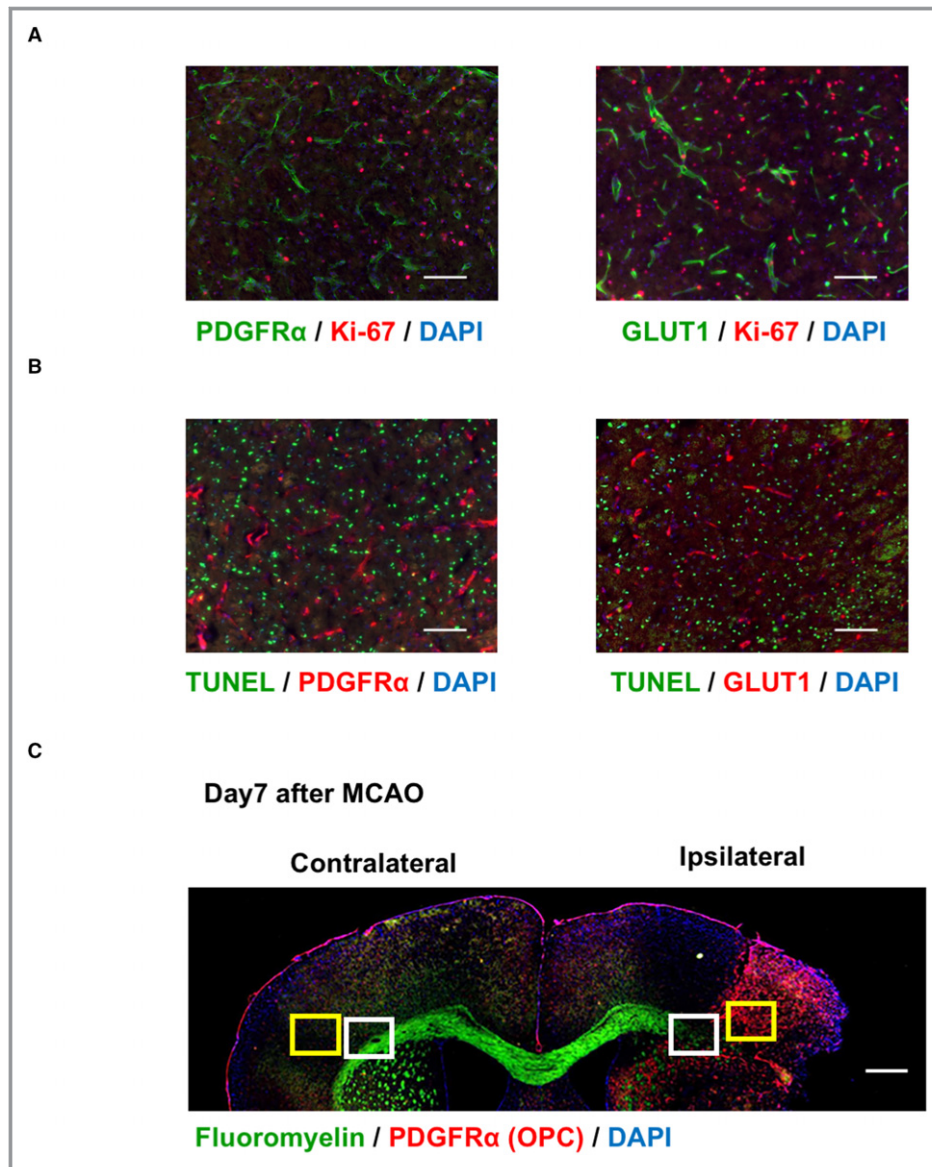
Figure 5. OPCs and endothelial cells display a certain degree of cell death and proliferation after cerebral ischemia. The additional OPCs that appeared after cerebral ischemia cannot overcome the myelin disruption on day 7 after MCAO. **A**, Representative images of Ki-67 with PDGFRα and GLUT1 immunostaining at the ischemic border area on day 7 after MCAO. Bar=100 μm. **B**, Representative images of TUNEL with PDGFRα and GLUT1 immunostaining at the ischemic border area on day 7 after MCAO. Bar=100 μm. **C**, Representative images of Fluoromyelin (green: marker for mature oligodendrocytes) and PDGFRα (marker for OPCs) immunostaining. Bar=400 μm. **D**, Histogram showing the fluorescent intensity of Fluoromyelin in the cerebral cortex and corpus callosum at the ipsilateral and contralateral sides on day 7 after MCAO. N=4 for each group. Data are analyzed using a Mann–Whitney test. $P<0.05$. DAPI indicates 4′,6-diamidino-2-phenylindole; GLUT1, glucose transporter 1; MCAO, middle cerebral artery occlusion; OPCs, oligodendrocyte precursor cells; PDGFRα, platelet-derived growth factor receptor-α; TUNEL, terminal deoxynucleotidyl transferase-mediated dUTP-biotin nick-end labeling.

Dunn test for pairwise comparison. Two-way repeated-measures ANOVA was used to compare variables in Garcia score. Results are represented as mean±SD. Statistical significance was defined as $P<0.05$.

Accession Numbers

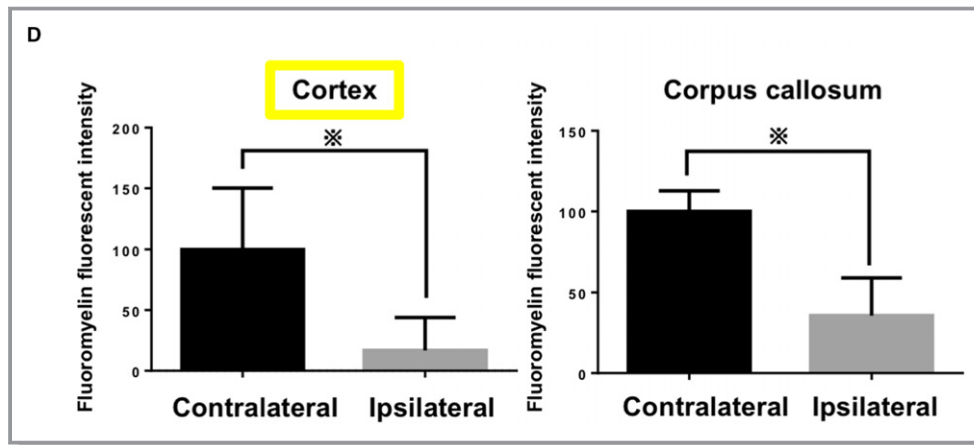The GEO accession number for the full data set of RNA-seq is 116409.

Figure 5. Continued

Results

Increased Perivascular OPCs in Cerebral Cortex and Striatum Coupled With Post-Stroke Angiogenesis After Cerebral Ischemia in Mice

As mentioned above, OPCs can be classified into 3 subtypes in the adult mouse brain according to their morphology and position in relation to cerebral endothelium: parenchymal OPCs, perivascular OPCs, and intermediate OPCs (Figure 1A).[8] Because PDGFR-α is a specific marker for OPCs in the brain,[20] co-staining of anti-PDGFR-α with anti-CD31 (endothelial cell marker) was performed to assess the OPC phenotypes. Perivascular OPCs completely wrap microvessels with their fine processes while parenchymal OPCs are localized away from microvessels. The intermediate OPCs have processes that are only partly located close to cerebral endothelium. Because the identification of the 3 subtypes of OPCs cannot be rigorous in a 2-dimensional image, we evaluated the subtypes of OPCs in a 3-dimensional image using a confocal laser-scanning microscope (Figure 1B). We first examined OPC phenotypic changes after ischemic stroke using a mouse model of stroke induced by transient MCAO. Strikingly, while the majority of OPCs are of the parenchymal subtype under normal conditions, an increase in number of perivascular OPCs was observed in the cerebral cortex 7 days after cerebral ischemia (Figure 1C). The increase in perivascular OPCs was observed at the border area within the ischemic core, defined as a microtubule-associated protein 2-negative area (Figure 1D), as well as hypoxyprobe-1-positive hypoxic area (Figure 1E). There were no significant changes in the OPC phenotypes in the ischemic penumbra, defined as a microtubule-associated protein 2-positive region (Figure 1D). PDGFRα-positive perivascular OPCs were not co-stained with PDGFRβ, Iba1, GFAP, nestin, or collagen-I, suggesting that perivascular OPCs can be distinguished from pericytes, macrophages/microglia, astrocytes, neural stem cells, and

fibroblasts (Figure 1F). Sholl analysis confirmed distinct morphological differences between parenchymal and perivascular OPCs (Figure 2). We further examined the temporal profiles of OPCs related to poststroke angiogenesis on day 1, 3, 7, 14, and 28 after MCAO (Figure 3A). As PDGFRα (+) fibronectin (+) fibrotic scar formation was observed on day 14 and 28 after cerebral ischemia (Figure 3B), the quantification of PDGFRα (+) OPCs in terms of perivascular versus parenchymal subsets was conducted on days 1, 3, and 7. The number of endothelial cells in the ischemic border area was decreased 1 day after cerebral ischemia. The number of endothelial cells then began to increase on day 3, and continued to show increases on day 7 (Figure 3A), which is in line with previous reports showing poststroke angiogenesis in the peri-infarct region 3 to 4 days following cerebral ischemia.[21] In parallel with poststroke angiogenesis, OPCs in the ischemic border area in the cerebral cortex were decreased 1 day after MCAO, but this number began to increase on day 3, and continued to show increases on day 7 (Figure 4A). The proportion of perivascular OPCs in the cerebral cortex reached a maximum on day 7 (accounting for 67% of all OPCs). Notably, the increase in perivascular OPCs was more pronounced in the cerebral cortex compared with that in corpus callosum (Figure 4A). The vascular density (as measured by GLUT1 fluorescent intensity) increased after MCAO, increases that were positively correlated with the number of perivascular OPCs in the cerebral cortex (Figure 4D). These results suggest that the growth of perivascular OPCs in the cerebral cortex is closely linked with poststroke angiogenesis. We also performed the co-staining of GLUT1 (endothelial cell marker) with Ki-67 (proliferation marker) and TUNEL (apoptosis marker). There were a small number of PDGFRα (+) Ki-67 (+) cells (proliferating OPCs; $2.8\pm1.4/0.25$ mm^2, N=4) and GLUT1 (+) Ki-67 (+) cells (proliferating endothelial cells; $2.0\pm1.1/0.25$ mm^2, N=4) on day 7 after MCAO (Figure 5A). Additionally, we identified a small number
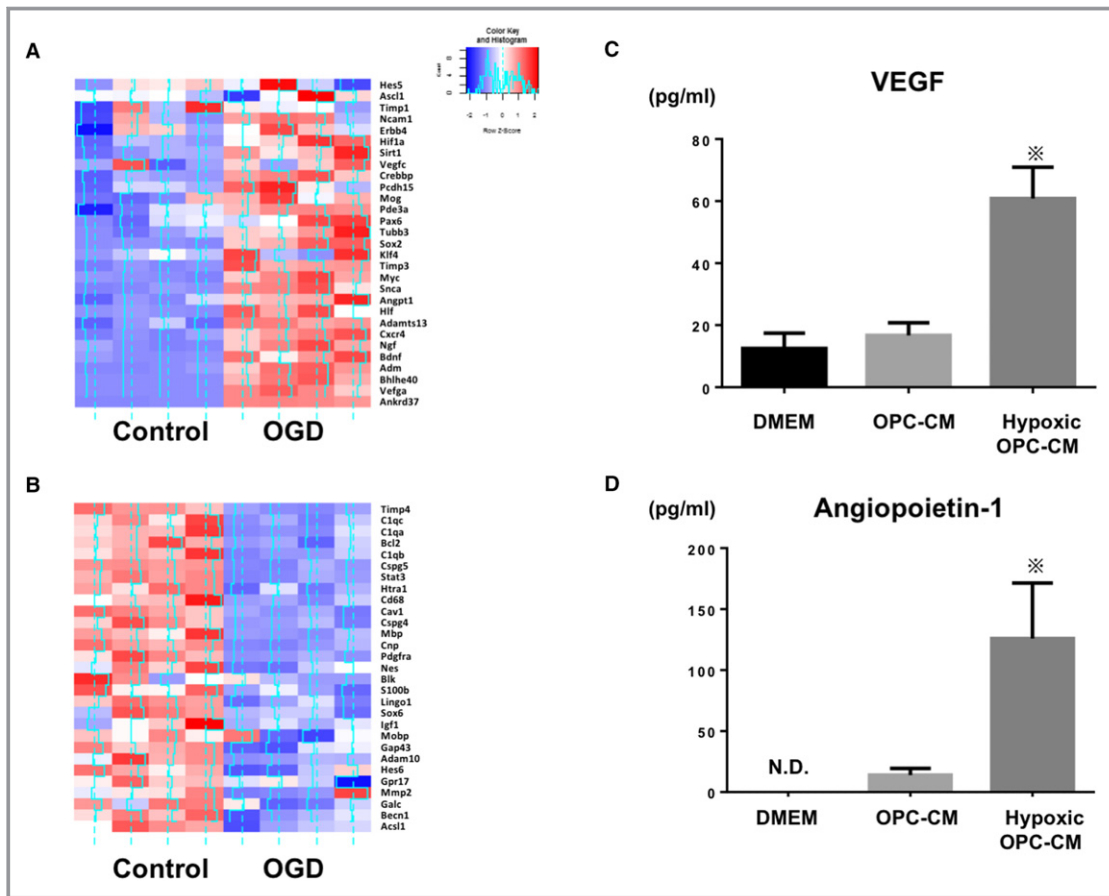
Figure 6. OPCs under hypoxic conditions increase pro-angiogenic factors in vitro. Hypoxic OPC-derived CM promotes angiogenesis in vitro. **A** and **B**, Heat map showing RNA-seq analysis of OPCs under normal conditions (control) and after OGD. **A**, The gene expressions of angiogenesis-promoting factors (**A**) such as *vegfa*, *angpt1*, and *adm* were upregulated, while those related to oligodendrocyte maturation such as *mbp*, *cnp*, and *gpr17* were suppressed (**B**), under severe hypoxic conditions. **C** and **D**, Histogram showing ELISA for the quantitative measurement of VEGF (**C**) and angiopoietin-1 (**D**) in DMEM (Dulbecco's modified Eagle medium), normoxic OPC-derived conditioned media (CM), and hypoxic OPC-derived CM (N=3 for each group). Data are analyzed using a Mann–Whitney test. *P*<0.05. **E**, In vitro media transfer experiment design. The tube formation of endothelial cells is evaluated after the transfer of OPC-derived media. **F**, Representative image of tube formation assay of DMEM-, normoxic OPC-CM-, and hypoxic OPC-CM-treated endothelial cells. **G** and **H**, Histogram showing the number of tube formations (**G**) and WST (cell viability) assay (**H**) of DMEM-, normoxic OPC-CM-, and hypoxic OPC-CM-treated endothelial cells (N=4 for each group). Data are expressed as the mean ±SD. Data are analyzed using a Kruskal–Wallis test. *P*<0.01. CM indicates conditioned media; N.D., not detected; OGD, oxygen glucose deprivation; OPCs, oligodendrocyte precursor cells; VEGF, vascular endothelial growth factor.

of PDGFRα (+) TUNEL (+) cells (dying OPCs; 2.5±1.3/ 0.25 mm^2, N=4) and GLUT1 (+) TUNEL (+) cells (dying endothelial cells; 1.6±0.4/0.25 mm^2, N=4) on day 7 after MCAO (Figure 5B). Thus, OPCs and endothelial cells display a certain degree of cell death and proliferation after cerebral ischemia. Meanwhile, the additional OPCs that appeared after cerebral ischemia could not overcome the myelin disruption in either the gray or the white matter on day 7 after MCAO, as evaluated by fluoromyelin staining, which revealed a decrease in myelin integrity at the ischemic area (Figure 5C and 5D). Collectively, the phenotypes of OPCs appear to dynamically shift from the parenchymal subtype to the perivascular

subtype after cerebral ischemia, and an increase in number of perivascular OPCs in the cerebral cortex is synchronized with poststroke angiogenesis in mice.

OPCs Under Hypoxic Condition Increase Pro-Angiogenic Factors In Vitro

Given our previous findings of increased hypoxia-induced perivascular OPCs and poststroke angiogenesis, we aimed to investigate the potential effects of these concomitant changes. First, to determine the phenotypic change of OPCs under hypoxic conditions, in detail, we evaluated the
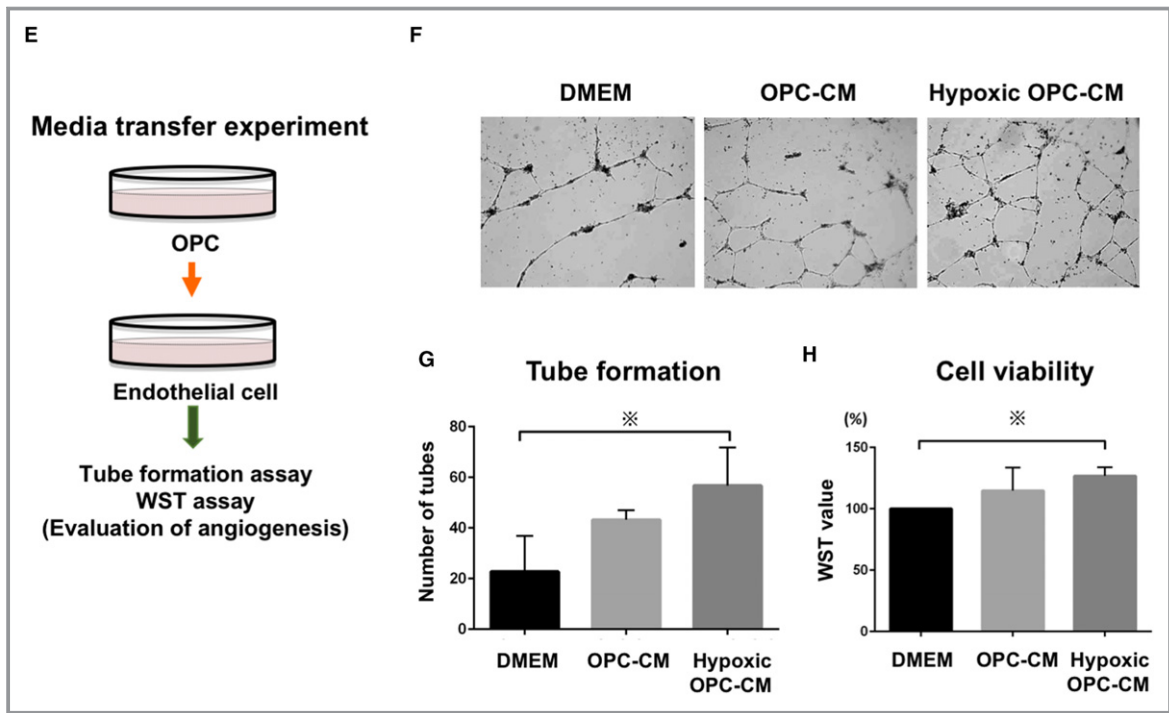
Figure 6. Continued

alterations of gene expressions in primary cultured OPCs after oxygen glucose deprivation. The cultured OPCs were obtained from neonatal rat cortex, the purity and functionality of which have been validated in our previous studies.[8,15,16] Notably, RNA-seq analysis of OPCs revealed substantial alterations in gene expression profiles 6 hours after oxygen glucose deprivation (0.1% oxygen). The gene expressions of angiogenesis-promoting factors such as *vegf*, *angpt1*, *wnt7*, and *adm* were upregulated, while those related to oligodendrocyte maturation such as *mbp*, *cnp*, and *gpr17* were suppressed, under severe hypoxic conditions (Figure 6A and 6B). To confirm whether these angiogenic factors are secreted into the media of OPCs, ELISA analysis was performed using the media derived from OPCs under normal and hypoxic conditions. To collect the media from OPCs without causing cell death, OPCs were subjected to 2% oxygen for 12 hours. Results of the analysis demonstrated that the concentrations of vascular endothelial growth factor (VEGF) and angiopoietin-1, in the media derived from hypoxic OPCs, were significantly increased (VEGF, 60.8 ± 10.1 pg/mL; angiopoietin-1, 126.0 ± 45.5 pg/mL) compared with the media derived from control OPCs (VEGF, 16.7 ± 4.1 pg/mL; angiopoietin-1, 13.9 ± 5.5pg/mL; Figure 6C and 6D). These results indicate that the OPC phenotype shifted towards pro-angiogenic after the hypoxic insult, and that the hypoxia-preconditioned OPCs (hypoxic OPCs) secrete a greater amount of angiogenic factors such as VEGF and angiopoietin-1.

Hypoxic OPC-Derived CM Promotes Angiogenesis In Vitro

To determine the functional consequences of OPC phenotypic changes and examine whether the hypoxic OPCs can indeed promote angiogenesis, we conducted media transfer experiments using OPCs and endothelial cells (Figure 6E). We found that hypoxic OPC-derived CM significantly increased the number of endothelial cell tube formations compared with OPC basal media, although normoxic OPC-CM did not show such positive effects (basal media versus OPC-CM versus hypoxic OPC-CM, 22.8 ± 14.1 versus 43.3 ± 3.8 versus 56.8 ± 15.1, $P<0.05$; Figure 6F and 6G). The WST assay also showed that treatment with hypoxic OPC-CM significantly increased the endothelial cell viability compared with OPC basal media (basal media versus OPC-CM versus hypoxic OPC-CM, 100% versus $114.8\pm19.3\%$ versus $126.8\pm7.4\%$, $P<0.05$; Figure 6H). Taken together, these results demonstrate that hypoxia-preconditioned OPCs promote angiogenesis via secreted factors in vitro.

Hypoxic OPC-Derived CM Promotes Angiogenesis In Vivo

Finally, given reports that the augmentation of poststroke angiogenesis may improve clinical outcomes after stroke, we investigated the therapeutic potential of hypoxic OPC-CM in cerebral ischemia. To determine whether hypoxic OPC-CM
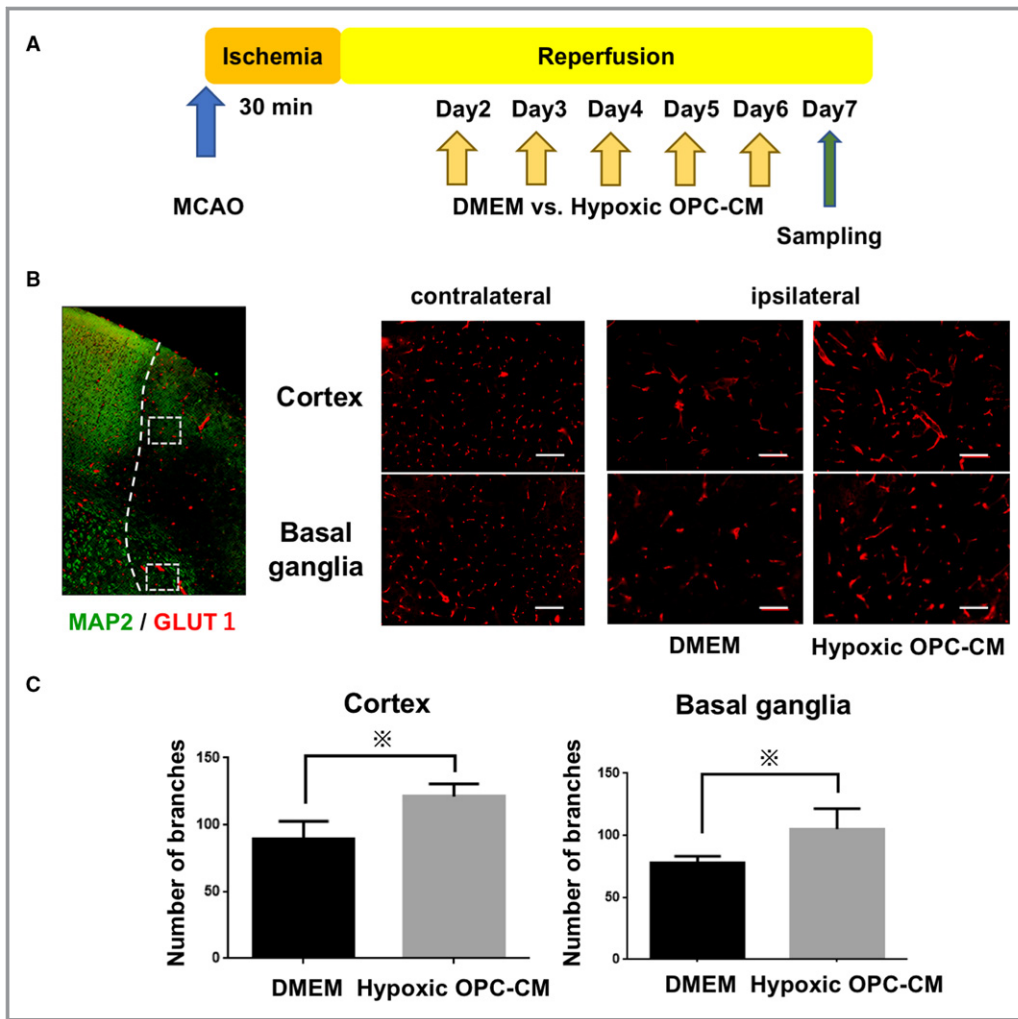
Figure 7. Five consecutive daily treatments with hypoxic OPC-derived CM promotes angiogenesis after MCAO in vivo. **A**, In vivo study design: DMEM (Dulbecco's modified Eagle medium) (as control) and nonconcentrated hypoxic OPC-CM were administered for 5 consecutive days beginning on the second day after MCAO. Histological and behavioral evaluation was conducted on the seventh day after MCAO. **B**, Representative images of GLUT1 (red: marker for endothelium) and MAP2 (green: marker for neuronal dendrites) immunostaining at the ischemic border area in the cerebral cortex and basal ganglia on day 7 after MCAO. Bar=100 μm. **C**, Histogram showing quantification of the number of the branches of endothelial cells at the ischemic border area in the cerebral cortex and basal ganglia. DMEM: N=5; hypoxic OPC-CM: N=6. Data are analyzed using a Mann–Whitney test. *P*<0.05. **D**, Representative images of IgG (red: marker for blood–brain barrier leakage) and GLUT-1 (green: marker for endothelial cells) of DMEM- and hypoxic OPC-CM-treated mice on day 7 after MCAO. Bar=100 μm. **E**, Histogram showing the fluorescent intensity of IgG staining at the ischemic border areas in DMEM- and hypoxic OPC-CM-treated mice on day 7 after MCAO. Data are represented by the mean±SD. N=4 for each group. Data are analyzed using a Mann–Whitney test. CM indicates conditioned media; GLUT-1, glucose transporter; MAP2, microtubule-associated protein 2; MCAO, middle cerebral artery occlusion; n.s., not significant; OPCs, oligodendrocyte precursor cells.

can promote poststroke angiogenesis and alleviate subsequent infarct volume and functional deterioration, we first intravenously injected DMEM (as control) and concentrated (5×) hypoxic OPC-CM on day 2 only once after reperfusion in mice exposed to 30 minutes of MCAO; the outcome of the injection was then assessed on day 7. Our results showed no significant difference in angiogenesis, infarct volume, or functional outcome between control and concentrated hypoxic OPC-CM-treated mice (data not shown). Therefore, we changed the therapeutic strategy as follows: consecutive 5-day intravenous injection of DMEM (vehicle) and nonconcentrated hypoxic OPC-CM were conducted beginning 2 days
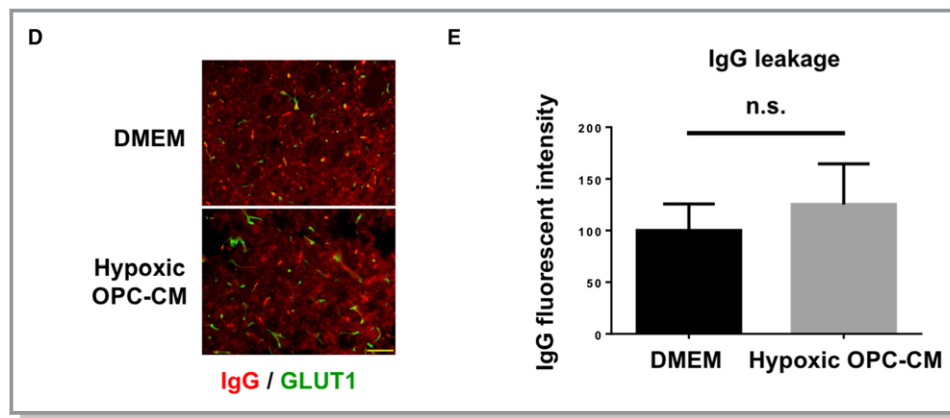
Figure 7. Continued

after MCAO (Figure 7A). On day 7 after MCAO, we assessed angiogenesis, neurogenesis, infarct volume, and motor function. Under this therapeutic protocol, 5 consecutive treatments with hypoxic OPC-CM promoted angiogenesis on day 7 after cerebral ischemia, as was demonstrated by the vascular density of GLUT-1-positive endothelial cells in the border area within the ischemic core (defined as a microtubule-associated protein 2-negative area) (vehicle versus hypoxic OPC-CM, 167.4 ± 16.75 versus 226.2 ± 23.62, $P<0.05$; Figure 7B and 7C). Because some angiogenic factors (such as VEGF) have detrimental effects on BBB integrity in addition to promoting angiogenesis, we evaluated BBB integrity after cerebral ischemia by means of IgG staining. There was no significant difference in BBB leakage between vehicle-treated mice and hypoxic OPC-CM-treated mice (Figure 7D and 7E). Additionally, because it has been reported that after the ischemia insult, neurogenesis and angiogenesis regenerative processes are coupled,[22] we evaluated poststroke neurogenesis by immunostaining with an antibody for doublecortin in the border area within the ischemic core. However, the density of the doublecortin-positive area was not significantly different between control and hypoxic OPC-CM-treated mice (data not shown). Nonetheless, infarct volume, assessed by Nissl staining, was reduced by the same treatment on day 7 after MCAO (control versus hypoxic OPC-CM, 0.581 ± 0.078 versus 0.475 ± 0.040, $P<0.05$; Figure 8A and 8B). Hypoxic OPC-CM-treated mice also showed a significant functional improvement ($P=0.0044$ in Garcia score, $P=0.011$ in neurological severity score) and a marginal improvement ($P=0.060$ in Rotarod test) with a significant reduction of body weight loss on day 7 after MCAO (Figure 8C and 8G). Taken together, 5 consecutive daily treatments with nonconcentrated hypoxic OPC-CM, beginning 2 days after MCAO, facilitate angiogenesis and reduce infarct volume possibly because of mechanisms other than augmented neurogenesis, leading to functional improvement.

Discussion

In this study, we demonstrated that (1) the phenotype of OPCs in the cerebral cortex shifts from the parenchymal subtype to the perivascular subtype after cerebral ischemia, and increases in the number of perivascular OPCs are synchronized with poststroke angiogenesis in mice; (2) the OPC phenotype becomes pro-angiogenic after hypoxic insult and hypoxia-preconditioned OPCs secrete a greater amount of angiogenic factors, such as VEGF and angiopoietin-1; (3) hypoxic OPCs promote vessel formation via secreted factors in vitro; and (4) 5 consecutive days of treatment with nonconcentrated hypoxic OPC-CM, beginning on the second day after MCAO, facilitates angiogenesis, alleviates infarct volume, and improves functional deficits after cerebral ischemia (Figure 9).

A recent study reported that OPC-expressed hypoxia-inducible factor promotes postnatal angiogenesis, but arrests OPC differentiation through secreted factors such as Wnt7, during the developmental stage.[23] Once the microvasculature is established, increased oxygen levels exert negative feedback on hypoxia-inducible factor activity, disinhibiting OPC maturation, which entails extraordinary metabolic demands.[23] The present study demonstrated that hypoxic insult shifts OPC phenotype to that of a perivascular subtype, which promotes poststroke angiogenesis along with decreased maturation capacity in the adult brain. Oxygen tension may be a key regulator for postnatal and poststroke angiogenesis and subsequent OPC maturation. Damaged adult brains partially exhibit a re-emergence of organizational patterns at the developmental stage,[24] while reactive OPCs may acquire new properties. Given that OPCs require the vascular scaffold for their migration during development,[25] the ischemia-induced perivascular OPCs at the ischemic border area might receive signals from vascular cells (including endothelial cells and pericytes), which may subsequently promote OPC
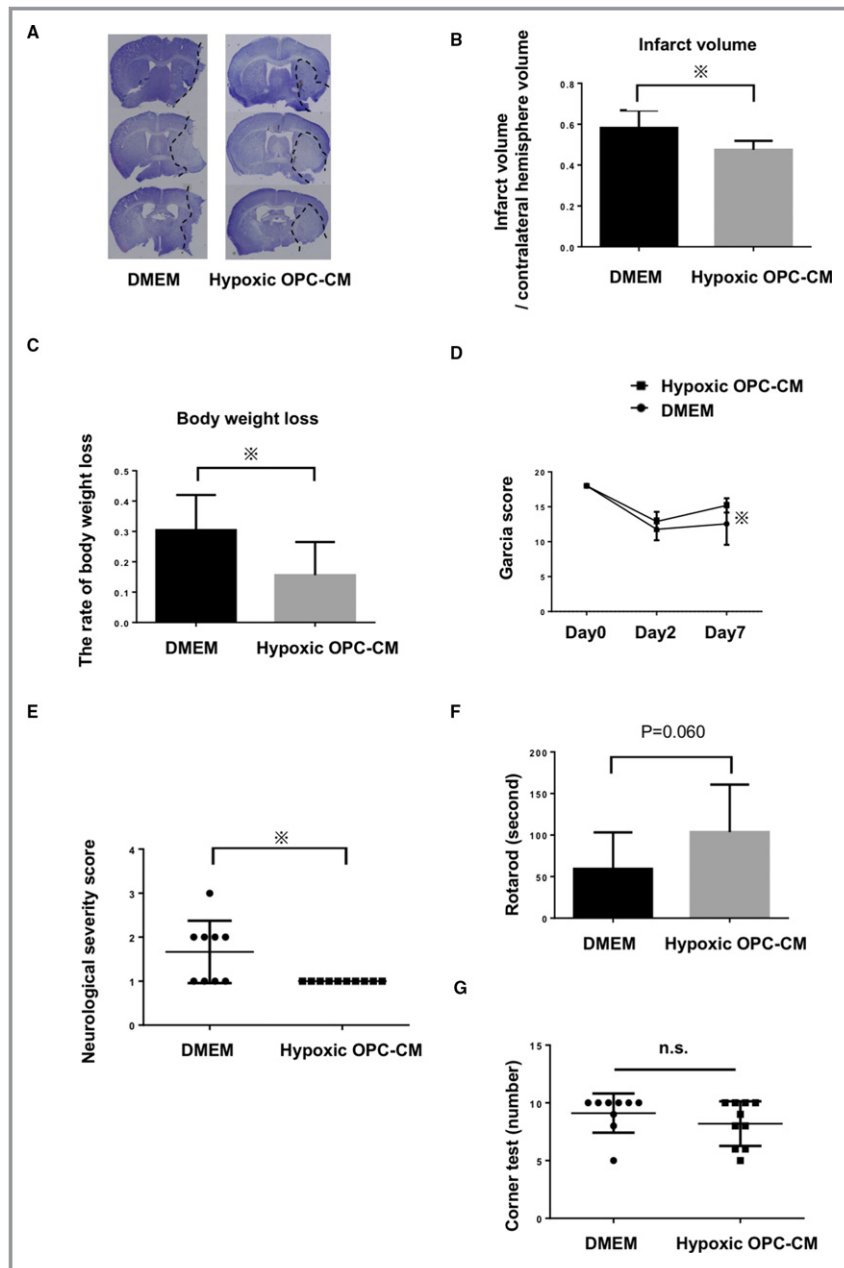
Figure 8. Five consecutive daily treatments with hypoxic OPC-derived CM alleviates infarct volume, and improves functional deficits in vivo. **A,** Representative images of Nissl staining. **B,** Histogram showing infarct volume ratio in Dulbecco's modified Eagle medium (DMEM)- and hypoxic OPC-CM-treated mice on day 7 after MCAO. Data are analyzed using a Mann–Whitney test. $P<0.05$. **C,** Histogram showing the rate of weight loss in DMEM- and hypoxic OPC-CM-treated mice on day 7 after MCAO. Data are represented by the mean±SD. DMEM: N=9; hypoxic OPC-CM: N=10. Data were analyzed using a Mann–Whitney test. $P<0.05$. **D,** Histogram showing the Garcia score, which reflects neurological deficits on days 2 and 7 after MCAO. Data are analyzed using a Mann–Whitney test. $P<0.01$. E-G, Histogram showing the neurological severity score (**E**), Rotarod (**F**), and corner test (**G**) in DMEM- and hypoxic OPC-CM-treated mice on day 7 after MCAO. DMEM: N=9; hypoxic OPC-CM: N=10. Data are represented by the mean±SD. The axis bar shows the median. NSS grade was analyzed using a Fisher exact test. Other data were analyzed using a Mann–Whitney test. $P<0.05$. n.s.=not significant. CM indicates conditioned media; MCAO, middle cerebral artery occlusion; NSS, neurological severity score; OPCs, oligodendrocyte precursor cells.
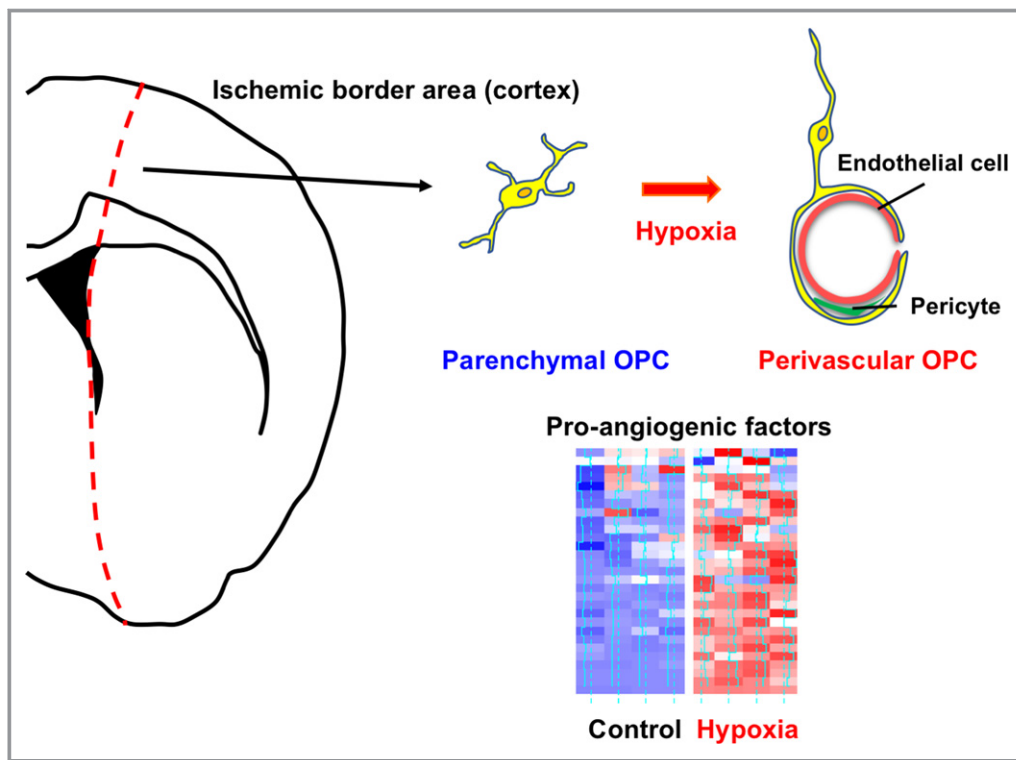
Figure 9. Schematic summary. We demonstrated that (1) OPCs in cerebral cortex shift to perivascular subtype after ischemia; (2) hypoxic OPCs express a number of pro-angiogenic factors; (3) hypoxic OPCs may promote poststroke angiogenesis; and (4) hypoxic OPCs secretome may provide a novel therapeutic option for stroke. OPCs indicates oligodendrocyte precursor cells.

migration and maturation.[26] Hence, the further elucidation of the similarities and differences of hypoxic OPCs at the developmental stage and in damaged adult brains would provide essential insights into efficient and inefficient OPC maturation and remyelination after brain injury.

There is a striking contrast in the phenotypic changes of OPCs, after cerebral ischemia, in gray and white matter regions. While OPCs in both cerebral gray and white matter demonstrated a shift to the perivascular subtype, this shift was much less pronounced in white matter OPCs. Differences in various properties of OPCs located in gray versus white matter have been previously reported. In terms of electrophysiological properties, OPCs located in white matter have a smaller capacitance, greater membrane resistance, and more depolarized resting membrane potential than OPCs located in gray matter.[27] In terms of cell cycling, OPCs located in white matter have a shorter cell division cycle than OPCs located in gray matter.[28] In addition, OPCs located in white matter have a greater proliferative response to PDGF-AA than OPCs located in gray matter without a significant difference in the expression of PDGFR-α at the perinatal stage.[29] Fate mapping studies show that while most of Olig2 (+) or PDGFR-α (+) OPCs located in white matter generate mature oligodendrocytes, in gray matter, most OPCs remain in an immature state,

even after injury.[30,31] Such undifferentiated OPCs in gray matter may have important functions beyond myelination. The present study demonstrated that OPCs located in the cerebral cortex have a higher capacity for promoting poststroke angiogenesis than OPCs located in white matter.

Therapeutic strategies for stroke should incorporate cerebral vasculature and the induction of angiogenesis.[21] This will not only provide ischemic brain tissue with oxygen and glucose, but it will also stimulate endogenous recovery including neuro-/oligodendrogenesis and neuronal/synaptic plasticity after ischemic injury. Furthermore, angiogenesis may have a salutary effect on the movements of inflammatory cells, which are charged with cleaning the postischemic environment.[21] However, the responses and regulatory mechanisms underlying angiogenesis in the brain are more complex than those in non–central nervous system tissues. The endothelial barrier function is severely compromised during the vascular remodeling process. For new vessels to evolve, the endothelial cell connections of the existing vasculature need to loosen to allow endothelial sprouting. For instance, VEGF, a well-established pro-angiogenic factor, triggers a cascade of aggravating events; BBB injury leads to edema formation and infarct increase in diabetic stroke,[32,33] while inducing angiogenesis. Enhanced vascular permeability

also increases the risk of hemorrhagic transformation, further aggravating the effects of stroke. Hence, the nature of angiogenesis, its beneficial time window, as well as the pathophysiological risk factors, need to be critically considered if angiogenesis is to be effectively incorporated into stroke therapies. The present study revealed that hypoxic OPC-CM contains multiple pro-angiogenic factors including VEGF as well as vessel-stabilizing factors such as angiopoietin-1 and adrenomedullin,[34] which could promote poststroke angiogenesis without enhancing BBB leakage. Optimal use of hypoxic OPCs secretome may be a promising therapeutic option for recovery of the neurovascular unit after stroke.

There are several caveats that can be addressed in future studies. First, we classified 3 subtypes of OPCs based on their location relative to vessels and their morphological features. Although we evaluated these 3 subtypes in a 3-dimensional image (Figure 1B), there remains a possibility of an inaccurate distinction between the "intermediate" OPCs and the other subtypes of OPCs. Thus, distinctive markers that can distinguish these subtypes of OPCs should be identified in future studies. Second, the source of increased perivascular OPCs after cerebral ischemia should be investigated in future studies. Some proliferating OPCs (PDGFRα (+) Ki-67 (+) cells) were observed on day 7 after MCAO (Figure 5A). Given that a recent study demonstrated that OPCs migrate along vasculature in the developmental brain, the proliferating OPCs may migrate into perivascular areas after cerebral ischemia. In order to confirm this point, we need to perform in vivo imaging of the mice that express a certain fluorescent protein specifically in OPCs for fate mapping of OPCs after cerebral ischemia. Furthermore, whether increased perivascular OPCs are derived from brain parenchyma or circulating blood should be elucidated in future studies. Third, the roles of endogenous hypoxic OPCs on angiogenesis after cerebral ischemia remain unproven, although correlation analysis suggests that the growth of perivascular OPCs in the cerebral cortex is closely linked with poststroke angiogenesis. A further loss-of-function approach is required to determine the role of endogenous OPCs on poststroke angiogenesis. Fourth, a recent single-cell RNA sequencing study revealed that there are 13 distinct populations of PDGFRα (+) cells, which exist in a region-dependent manner, in the juvenile and adult mouse brain.[4] Although the present study demonstrated phenotypic differences between OPCs located in the cerebral cortex versus the corpus callosum after cerebral ischemia, detailed regional and subregional differences in OPC phenotypes after brain injury could be further elucidated by conducting a genome-wide analysis of OPCs from discrete brain regions and monitoring OPC reactivity in disease. Fifth, although we demonstrated the therapeutic potential of hypoxic OPC-CM in stroke, the detailed underlying mechanisms and mediating factors have not yet been identified. Deciphering the mechanisms that are responsible for hypoxic OPC-mediated positive effects would contribute to the development of a targeted therapy for stroke.

In conclusion, cerebral ischemia shifts the phenotype of OPCs in the cerebral cortex to that of a perivascular subtype, which promotes angiogenesis. Optimal use of hypoxic OPCs, which can facilitate functional angiogenesis after cerebral ischemia, without exacerbating BBB leakage, would provide a novel therapeutic option for stroke. Considering the harmonized orchestration of all cell types in a disease is fundamental for minimizing damage and augmenting recovery. Thus, further studies examining OPC diversity and interaction with other cell types, in the context of various central nervous system diseases, are warranted.

Sources of Funding

Disclosures

None.

References

1. Moskowitz MA, Lo EH, Iadecola C. The science of stroke: mechanisms in search of treatments. *Neuron*. 2010;67:181–198.

2. Lo EH. Degeneration and repair in central nervous system disease. *Nat Med*. 2010;16:1205–1209.

3. Maki T, Hayakawa K, Pham LD, Xing C, Lo EH, Arai K. Biphasic mechanisms of neurovascular unit injury and protection in CNS diseases. *CNS Neurol Disord Drug Targets*. 2013;12:302–315.

4. Marques S, Zeisel A, Codeluppi S, van Bruggen D, Mendanha Falcao A, Xiao L, Li H, Haring M, Hochgerner H, Romanov RA, Gyllborg D, Munoz Manchado A, La Manno G, Lonnerberg P, Floriddia EM, Rezayee F, Ernfors P, Arenas E, Hjerling-Leffler J, Harkany T, Richardson WD, Linnarsson S, Castelo-Branco G. Oligodendrocyte heterogeneity in the mouse juvenile and adult central nervous system. *Science*. 2016;352:1326–1329.

5. Ben Haim L, Rowitch DH. Functional diversity of astrocytes in neural circuit regulation. *Nat Rev Neurosci*. 2017;18:31–41.

6. Grabert K, Michoel T, Karavolos MH, Clohisey S, Baillie JK, Stevens MP, Freeman TC, Summers KM, McColl BW. Microglial brain region-dependent diversity and selective regional sensitivities to aging. *Nat Neurosci*. 2016;19:504–516.

7. Dimou L, Simons M. Diversity of oligodendrocytes and their progenitors. *Curr Opin Neurobiol*. 2017;47:73–79.

8. Maki T, Maeda M, Uemura M, Lo EK, Terasaki Y, Liang AC, Shindo A, Choi YK, Taguchi A, Matsuyama T, Takahashi R, Ihara M, Arai K. Potential interactions between pericytes and oligodendrocyte precursor cells in perivascular regions of cerebral white matter. *Neurosci Lett*. 2015;597:164–169.

9. Seo JH, Maki T, Maeda M, Miyamoto N, Liang AC, Hayakawa K, Pham LD, Suwa F, Taguchi A, Matsuyama T, Ihara M, Kim KW, Lo EH, Arai K. Oligodendrocyte precursor cells support blood-brain barrier integrity via TGF-beta signaling. *PLoS ONE*. 2014;9:e103174.

10. Miyamoto N, Maki T, Shindo A, Liang AC, Maeda M, Egawa N, Itoh K, Lo EK, Lok J, Ihara M, Arai K. Astrocytes promote oligodendrogenesis after white matter damage via brain-derived neurotrophic factor. *J Neurosci*. 2015;35:14002–14008.

11. Hara H, Huang PL, Panahian N, Fishman MC, Moskowitz MA. Reduced brain edema and infarction volume in mice lacking the neuronal isoform of nitric oxide synthase after transient MCA occlusion. *J Cereb Blood Flow Metab*. 1996;16:605–611.

12. Choi YK, Maki T, Mandeville ET, Koh SH, Hayakawa K, Arai K, Kim YM, Whalen MJ, Xing C, Wang X, Kim KW, Lo EH. Dual effects of carbon monoxide on pericytes and neurogenesis in traumatic brain injury. *Nat Med*. 2016;22:1335–1341.

13. Garcia JH, Wagner S, Liu KF, Hu XJ. Neurological deficit and extent of neuronal necrosis attributable to middle cerebral artery occlusion in rats. Statistical validation. *Stroke*. 1995;26:627–634; discussion 635.

14. Rajasekharan S, Baker KA, Horn KE, Jarjour AA, Antel JP, Kennedy TE. Netrin 1 and dcc regulate oligodendrocyte process branching and membrane extension via Fyn and RhoA. *Development*. 2009;136:415–426.

15. Maki T, Takahashi Y, Miyamoto N, Liang AC, Ihara M, Lo EH, Arai K. Adrenomedullin promotes differentiation of oligodendrocyte precursor cells into myelin-basic-protein expressing oligodendrocytes under pathological conditions in vitro. *Stem Cell Res*. 2015;15:68–74.

16. Kaji S, Maki T, Kinoshita H, Uemura N, Ayaki T, Kawamoto Y, Furuta T, Urushitani M, Hasegawa M, Kinoshita Y, Ono Y, Mao X, Quach TH, Iwai K, Dawson VL, Dawson TM, Takahashi R. Pathological endogenous alpha-synuclein accumulation in oligodendrocyte precursor cells potentially induces inclusions in multiple system atrophy. *Stem Cell Reports*. 2018;10:356–365.

17. Maki T, Morancho A, Martinez-San Segundo P, Hayakawa K, Takase H, Liang AC, Gabriel-Salazar M, Medina-Gutierrez E, Washida K, Montaner J, Lok J, Lo EH, Arai K, Rosell A. Endothelial progenitor cell secretome and oligovascular repair in a mouse model of prolonged cerebral hypoperfusion. *Stroke*. 2018;49:1003–1010.

18. Bolger AM, Lohse M, Usadel B. Trimmomatic: a flexible trimmer for illumina sequence data. *Bioinformatics*. 2014;30:2114–2120.

19. Dobin A, Davis CA, Schlesinger F, Drenkow J, Zaleski C, Jha S, Batut P, Chaisson M, Gingeras TR. Star: ultrafast universal RNA-seq aligner. *Bioinformatics*. 2013;29:15–21.

20. Sim FJ, McClain CR, Schanz SJ, Protack TL, Windrem MS, Goldman SA. Cd140a identifies a population of highly myelinogenic, migration-competent and efficiently engrafting human oligodendrocyte progenitor cells. *Nat Biotechnol*. 2011;29:934–941.

21. Beck H, Plate KH. Angiogenesis after cerebral ischemia. *Acta Neuropathol*. 2009;117:481–496.

22. Ruan L, Wang B, ZhuGe Q, Jin K. Coupling of neurogenesis and angiogenesis after ischemic stroke. *Brain Res*. 2015;1623:166–173.

23. Yuen TJ, Silbereis JC, Griveau A, Chang SM, Daneman R, Fancy SPJ, Zahed H, Maltepe E, Rowitch DH. Oligodendrocyte-encoded HIF function couples postnatal myelination and white matter angiogenesis. *Cell*. 2014;158:383–396.

24. John GR, Shankar SL, Shafit-Zagardo B, Massimi A, Lee SC, Raine CS, Brosnan CF. Multiple sclerosis: re-expression of a developmental pathway that restricts oligodendrocyte maturation. *Nat Med*. 2002;8:1115–1121.

25. Tsai HH, Niu J, Munji R, Davalos D, Chang J, Zhang H, Tien AC, Kuo CJ, Chan JR, Daneman R, Fancy SP. Oligodendrocyte precursors migrate along vasculature in the developing nervous system. *Science*. 2016;351:379–384.

26. Kokovay E, Goderie S, Wang Y, Lotz S, Lin G, Sun Y, Roysam B, Shen Q, Temple S. Adult SVZ lineage cells home to and leave the vascular niche via differential responses to SDF1/CXCR4 signaling. *Cell Stem Cell*. 2010;7:163–173.

27. Larson VA, Zhang Y, Bergles DE. Electrophysiological properties of NG2(+) cells: matching physiological studies with gene expression profiles. *Brain Res*. 2016;1638:138–160.

28. Young KM, Psachoulia K, Tripathi RB, Dunn SJ, Cossell L, Attwell D, Tohyama K, Richardson WD. Oligodendrocyte dynamics in the healthy adult CNS: evidence for myelin remodeling. *Neuron*. 2013;77:873–885.

29. Hill RA, Patel KD, Medved J, Reiss AM, Nishiyama A. Ng2 cells in white matter but not gray matter proliferate in response to PDGF. *J Neurosci*. 2013;33:14558–14566.

30. Dimou L, Simon C, Kirchhoff F, Takebayashi H, Gotz M. Progeny of Olig2-expressing progenitors in the gray and white matter of the adult mouse cerebral cortex. *J Neurosci*. 2008;28:10434–10442.

31. Rivers LE, Young KM, Rizzi M, Jamen F, Psachoulia K, Wade A, Kessaris N, Richardson WD. PDGFRA/NG2 glia generate myelinating oligodendrocytes and piriform projection neurons in adult mice. *Nat Neurosci*. 2008;11:1392–1401.

32. Reeson P, Tennant KA, Gerrow K, Wang J, Weiser Novak S, Thompson K, Lockhart KL, Holmes A, Nahirney PC, Brown CE. Delayed inhibition of VEGF signaling after stroke attenuates blood-brain barrier breakdown and improves functional recovery in a comorbidity-dependent manner. *J Neurosci*. 2015;35:5128–5143.

33. Kim E, Yang J, Park KW, Cho S. Inhibition of VEGF signaling reduces diabetes-exacerbated brain swelling, but not infarct size, in large cerebral infarction in mice. *Transl Stroke Res*. 2018;9:540–548.

34. Maki T, Ihara M, Fujita Y, Nambu T, Miyashita K, Yamada M, Washida K, Nishio K, Ito H, Harada H, Yokoi H, Arai H, Itoh H, Nakao K, Takahashi R, Tomimoto H. Angiogenic and vasoprotective effects of adrenomedullin on prevention of cognitive decline after chronic cerebral hypoperfusion in mice. *Stroke*. 2011;42:1122–1128.